PARTICLE PRODUCTION BY NEUTRINOS

P. Schreiner
Argonne National Laboratory
Argonne, Illinois 60439

This paper is a review of particle production by neutrinos in charged-current inclusive and exclusive channels. In Fig. 1, I have compared the production rates for various particles in neutrino-nucleon interactions at a beam energy of 25 GeV. The mesons are, of course, dominated by pion production. The $\rho^o(760)$ rate is an order of magnitude smaller. Strange and charm pseudoscalar mesons are a further factor of two down in rate. The strange vector mesons are suppressed by more than an order of magnitude relative to K^o production; however, the charmed $D^{*+}(2010)$ is only a factor of two smaller in rate than the $D^o(1860)$. With regards to the baryons, most of them are, of course, nucleons. The Λ^o and $Y^*(1385)$ rates are down by one and two orders of magnitudes, respectively. The lower limit on the charmed Σ_c^{++} baryon rate is similar to the $Y^*(1385)$ rate. Finally, the quasielastic and one-pion production exclusive channels have about the same cross section as that of the D^{*+}; associated production of strange particles in the $\nu n \to \mu^- K^+ \Lambda$ channel and the $\Delta S = +\Delta Q$ process $\nu p \to \mu^- p K^+$ are down by factors of five and twenty, respectively, compared to the quasielastic cross section.

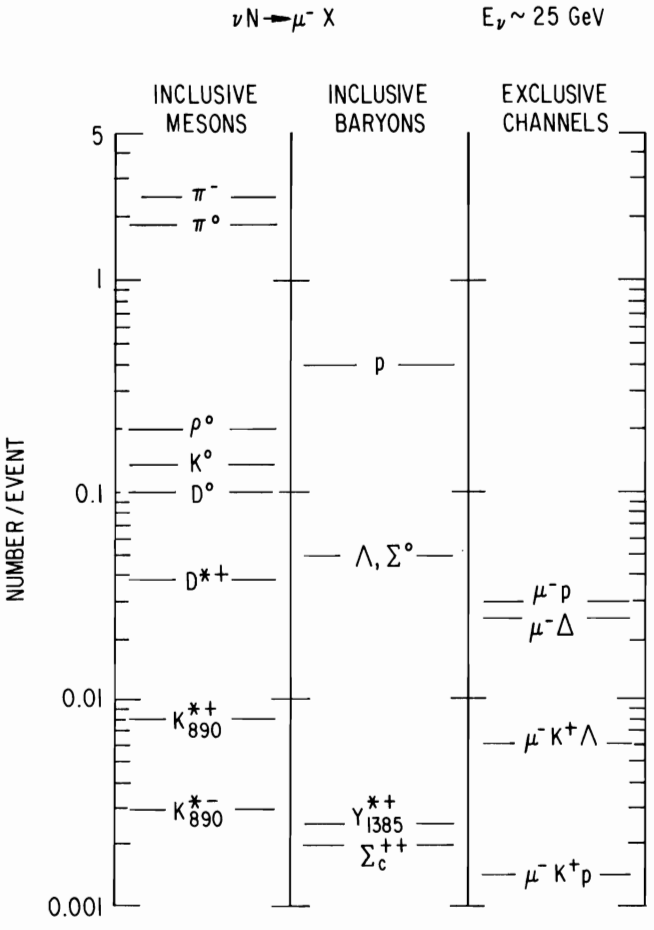

Fig. 1 Comparison of particle production rates per event in neutrino-nucleon collisions at $E_\nu \sim 25$ GeV.

I will, in order of increasing mass, review the new data available on some of these processes.

Low Mass Particles

One-pion production is the only inelastic neutrino process with good data available and corresponding detailed theoretical calculations. There are three neutrino and three corresponding antineutrino one-pion production reactions. As shown in Table I, the amplitudes for the reactions can be decomposed into isospin 1/2 and isospin 3/2 components, with ϕ_{13} being the relative phase angle between them. One basic physics goal of the experiments is to measure these amplitudes as a function of πN mass. What is usually measured are the πN mass spectrum, the cross section for any observed bumps in the mass spectrum, and some corresponding production and decay angular distributions.

Table II gives a summary of the six recent experiments.[1-6] The typical experiment has a few hundred events available in any channel.

Figure 2(a-b) shows the $p\pi^+$ effective mass distribution in the three-constraint process $\nu p \to \mu^- p\pi^+$ for mean beam energies of 1 and 30 GeV; the data are from the 12-foot[1] and BEBC[4] light liquid experiments. At low energy, only the $\Delta^{++}(1236)$

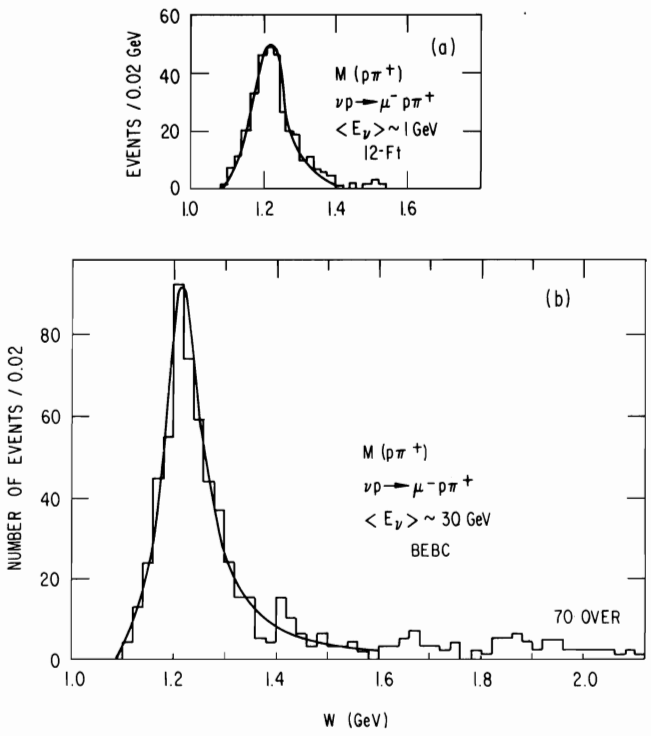

Fig. 2 The $p\pi^+$ effective mass distribution in the reaction $\nu p \to \mu^- p\pi^+$ as measured in the (a) ANL-CMU-Purdue 12-ft deuterium experiment and (b) the Aachen-Bonn-CERN-Munich-Oxford BEBC hydrogen experiment.

Table I: One Pion Production Amplitudes

One Pion Production	Reactions	Isovector Amplitudes
$\nu p \to \mu^- p\pi^+$	$\bar{\nu} n \to \mu^+ n\pi^-$	$T_{3/2}$
$\nu n \to \mu^- p\pi^o$	$\bar{\nu} p \to \mu^+ n\pi^o$	$\frac{\sqrt{2}}{3} T_{3/2} - \frac{\sqrt{2}}{3} T_{1/2}$
$\nu n \to \mu^- n\pi^+$	$\bar{\nu} p \to \mu^+ p\pi^-$	$\frac{1}{3} T_{3/2} + \frac{2}{3} T_{1/2}$

Table II: Summary of Recent One Pion Production Experiments

Experiment	Bubble Chamber	E (GeV)	Reactions	Σ Events
ACMP[1]	12-foot/D_2	0.5 - 6	$\nu N \to \mu^- N\pi$	600
ABCED[2]	GGM/Propane + Freon	1 - 8	$\nu N \to \mu^- N\pi$	~ 600
BMSTL[3]	GGM/Propane + Freon	1 - 8	$\bar{\nu} N \to \mu^+ N\pi$	~650
ABCMO[4]	BEBC/H_2	5 - 100	$\nu p \to \mu^- p\pi^+$	700
FMBH[5]	15-foot/H_2	5 - 100	$\nu p \to \mu^- p\pi^+$	200
ACMP[6]	15-foot/H_2	5 - 80	$\bar{\nu} p \to \mu^+ p\pi^-$	130

state is visible. At high energy, there are events at high mass, but no peaks are apparent in the 1700 or 1900 MeV mass regions where several Δ states are known to exist. The I = 3/2 Nπ amplitude at high mass is certainly not large.

Figure 3(a-b) shows the $p\pi^-$ effective mass distribution in the three-constraint process $\bar{\nu} p \to \mu^+ p\pi^-$ for mean beam energies of 3 and 25 GeV; the data are from GGM[3] and the 15-foot chamber[6] experiments. Even at low energy, there is considerable production of events with mass greater than 1.4 GeV. With the energy increased to ~ 25 GeV, the $\Delta^o(1236)$ is hardly visible; the mass spectrum is dominated by the 1400-1900 MeV region. Since we know the I = 3/2 amplitude is small for $M_{N\pi} > 1.4$ GeV, the I = 1/2 amplitude must be responsible for this broad enhancement.

Figure 4(a) shows the energy dependence of the $\nu p \to \mu^- \Delta^{++}$ cross section from 0.5 to 100 GeV. The data displayed are from three different bubble chambers.[1,4,5] The neutrino flux was determined by pion and kaon yields for the 12-foot data. The other two experiments have determined the flux by normalizing their inclusive data sample to the measured νN total cross section and using the QPM to fix the neutron/proton cross section ratio. The three experiments are in good agreement on the $\mu^- \Delta^{++}$ cross section; for $E_\nu > 5$ GeV, $\sigma = (0.64 \pm 0.03) \times 10^{-38}$ cm^2. Adler's model[7] with $M_A = 1.05$ GeV, and several quark models[8-10], give good fits to the data. Fig. 4(b) shows the energy dependence of the $\bar{\nu} p \to \mu^+ p\pi^-$ cross section[3,6] for $M_{p\pi^-} < 1.9$ GeV. This mass selection presumably selects several N^* states along with the $\Delta^o(1236)$. The slow rise of the cross section is due to (1) destructive inter-

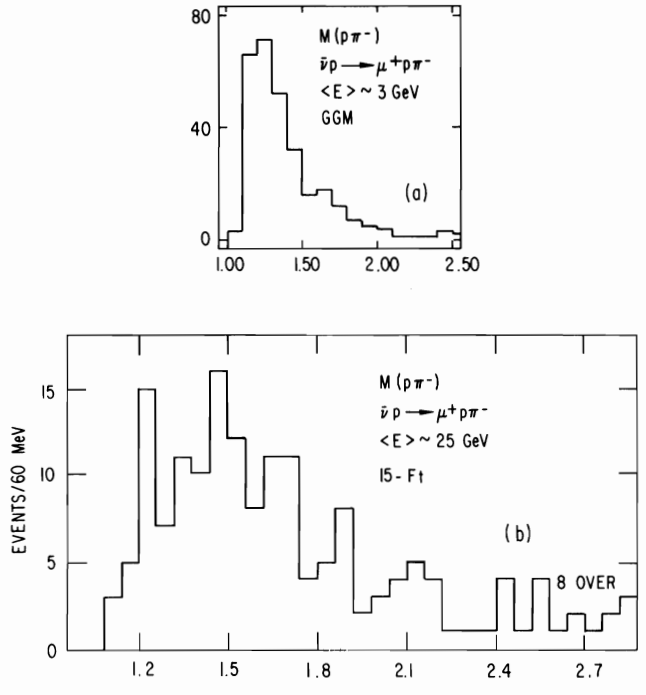

Fig. 3 The $p\pi^-$ effective mass distribution in the reaction $\bar{\nu} p \to \mu^+ p\pi^-$ as measured in the (a) GGM propane-freon experiment and (b) the Argonne-Carnegie-Mellon-Purdue 15-ft hydrogen experiment.

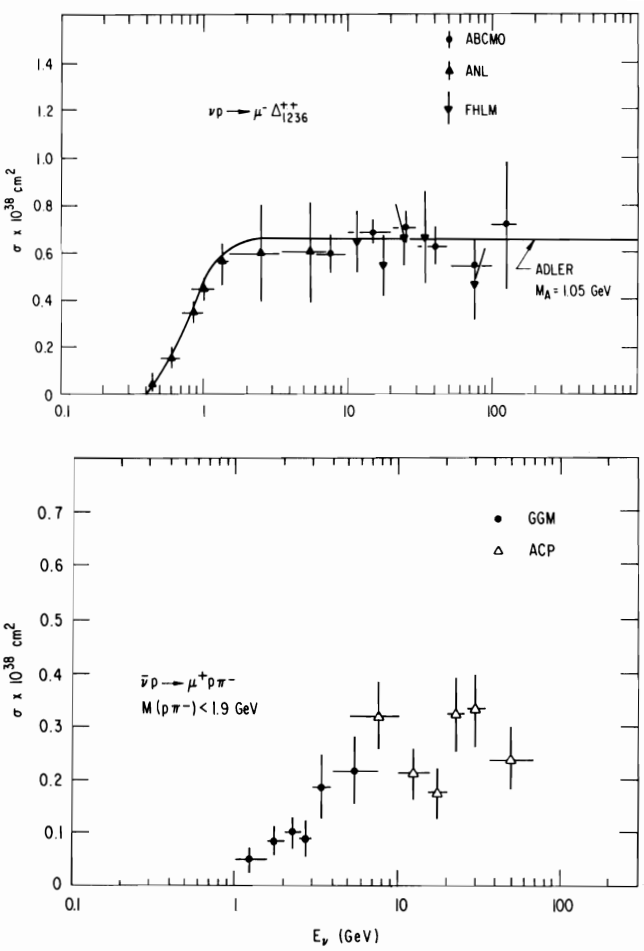

Fig. 4 (a) Energy dependence of the $\nu p \rightarrow \mu^- \Delta^{++}_{1236}$ cross section as measured in three bubble chambers. The curve is the Adler model[7] prediction with M_A set at 1.05 GeV. (b) Energy dependence of the $\bar{\nu} p \rightarrow \mu^+ p \pi^-$ cross section, for $M_{p\pi^-} < 1.9$ GeV, as measured in two bubble chamber experiments. See Table II for details of the experiments.

ference between the vector and axial amplitudes and (2) new N^* thresholds being crossed as the energy increases. One would expect the cross section to become flat at high energy; the data is consistent with that hypothesis, but cannot yet be proved. For $E_\nu \gtrsim 10$ GeV, $\sigma(\mu^+ p \pi^-) \approx 0.25 \times 10^{-38}$ cm^2. This value is in fair agreement with quark model predictions.[8-10] Likewise, if one determines a rate for the 1.6 - 1.8 GeV and 1.8 - 2.0 GeV $p\pi^+$ effective mass regions by assuming a 30% $N\pi$ branching ratio for the typical N^{*++} state, then the result of 0.1×10^{-38} cm^2 for both regions is also in rough agreement with quark model predictions.

It is clear that N^* and Δ spectroscopy with neutrino beams is difficult. Only the $\Delta(1236)$ has been clearly seen, although other higher mass states are certainly being produced.

In the energy region below 8 GeV, several experiments[1-3] have extracted the isospin 1/2 and 3/2 amplitudes. Figure 5 compares amplitude results from three low energy experiments using the 12-foot and GGM chambers (see Table II for details). Be-

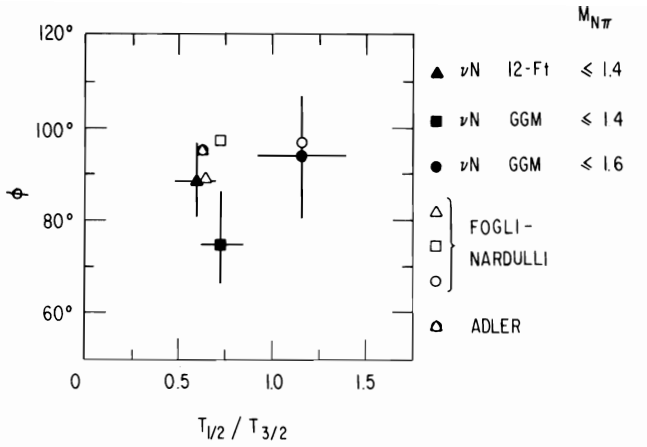

Fig. 5 Results for $T_{1/2}/T_{3/2}$ and the phase angle ϕ from three of the one-pion production experiments listed in Table II. The open points are the corresponding predictions of the Fogli-Nardulli quark model.[8] A prediction of the Adler model for the 12-ft data is also shown.

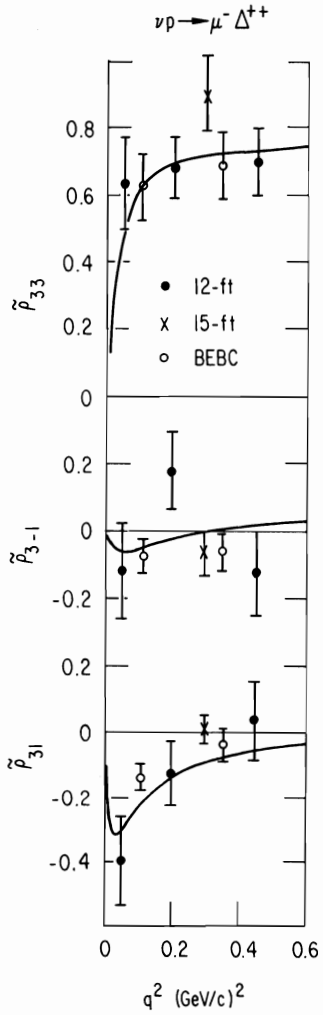

Fig. 6 The measured Δ^{++}_{1236} decay density matrix elements from three of the experiments listed in Table II. The curves are the predictions of the Adler model for the low energy 12-ft experiment; however, the predictions are nearly the same at 30 GeV.

cause the beam spectra and experimental cuts differ between experiments, some differences in the results are expected. Nevertheless, there seems to be agreement that the I = 1/2 amplitude is large even at low Nπ effective mass, and that the relative phase angle is near 90°. The open points in the figures are predictions of the Fogli-Nardulli quark model[8] where attention was paid to the experimental conditions of each experiment.

The agreement with data is very good in two cases, and only two standard deviations off for the GGM νN results. The Adler prediction[7] is also shown for the 12-foot case and the agreement is fine.

Additional information on the Δ(1236) form factors can be obtained from the production and decay angular distributions. Figure 6 shows the three $\Delta^{++}(1236)$ decay density matrix elements as a function of Q^2 using data from the low energy 12-foot experiment[1] and the high energy BEBC and 15-foot experiments.[4,5] Also shown is the Adler prediction[7] as calculated for the 12-foot experiment. However, the decay distributions are predicted to be nearly energy-independent so the curves may also be compared with the ~ 30 GeV data. The experiments and model seem to be in fairly good agreement. The FMBH group claims to see some "illegal" angular moments in the Δ decay, implying the presence of non-resonant background in the final state. This effect still needs to be confirmed.

Finally, Fig. 7 shows the dN/dQ^2 distribution[1] for the three neutrino reactions at low energy. There is fairly good agreement with Adler's prediction, although one would like better data on the $\mu^- p\pi^0$ channel. Figure 8 shows $d\sigma/dQ^2$ for the $\nu p \to \mu^- \Delta^{++}$ process at high energy. The 15-foot[5] and BEBC[4] data are in very good agreement. The predictions of Adler with $M_A = 1.05$ GeV and the Fogli quark model (nearly identical) do not agree well with the data. Note that the $Q^2 = 0$ point is constrained by PCAC, and that the high Q^2 curve is dominated by the vector amplitudes. One can, of course, change the value of M_A to improve the prediction, but the σ_T prediction would then not be as good.

It should be remembered that there is little previous data on exclusive neutrino reactions for $Q^2 \geq 1.5$ (GeV/c)^2 and that no neutrino experiment has ever made a quantitative measurement of a form factor. Even for quasielastic scattering, $\nu n \to \mu^- p$, the available data can be equally well fit by a monopole, dipole, and a quark model-vector dominance shape. This is shown in Fig. 9. So it is not surprising that the low energy models do not correctly predict the shape of the high Q^2 distribution.

We can now summarize the one-pion production data:
- the experiments are in reasonable agreement on $M_{N\pi}$, dN/dQ^2, ρ_{mn}, and σ_T measurements.
- the I = 1/2 amplitude is large for all $M_{N\pi} \leq 1.9$ GeV.

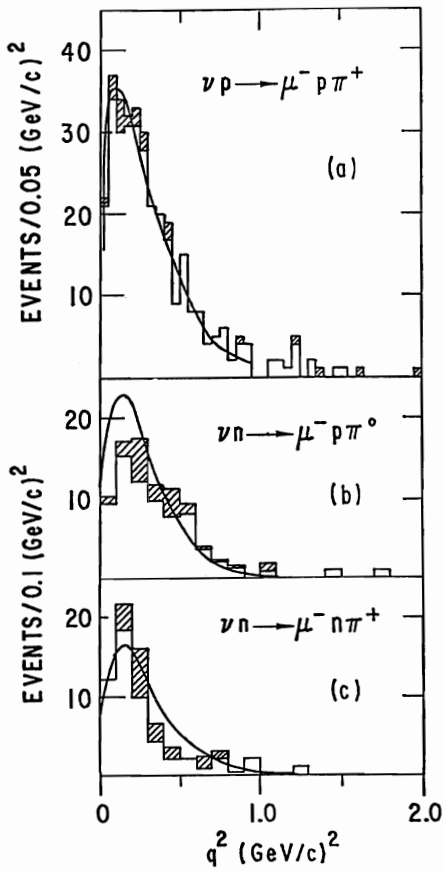

Fig. 7 dN/dQ^2 for three neutrino-induced one pion channels as measured in the low energy 12-ft experiment. The curves are the Adler model predictions.

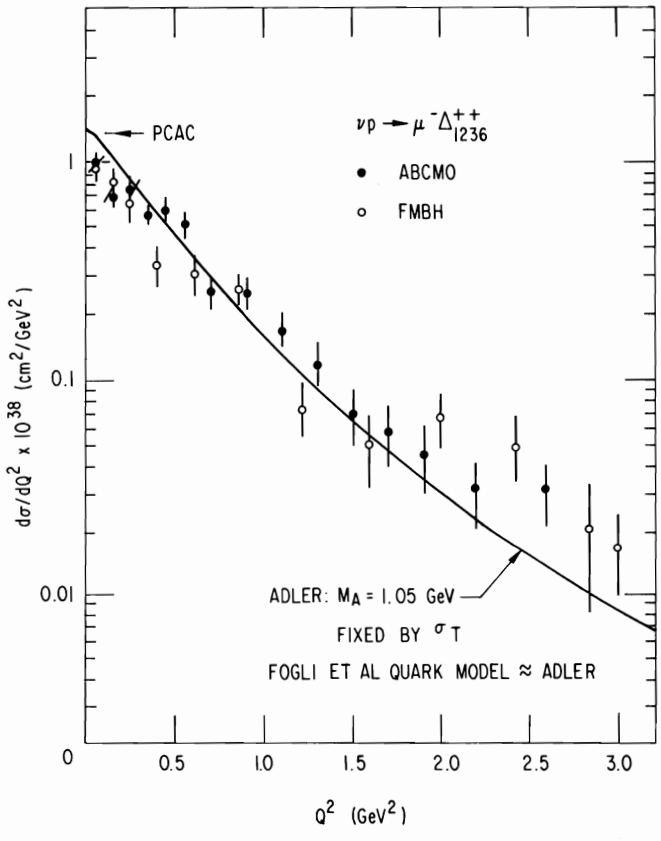

Fig. 8 $d\sigma/dQ^2$ for $\nu p \to \mu^- \Delta^{++}$ as measured in the 15-ft FMBH experiment and in the BEBC ABCMO experiment. The curve is the Adler model prediction with $M_A = 1.05$ GeV.

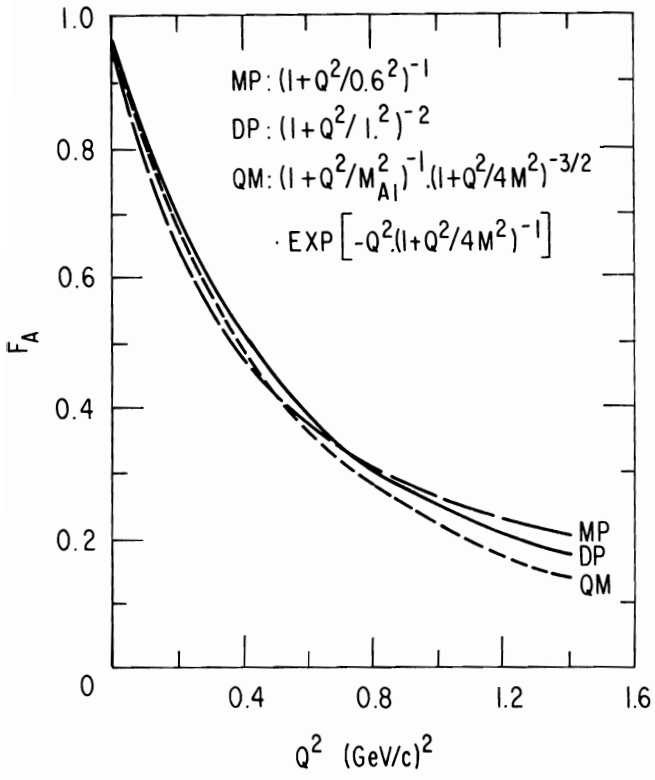

Fig. 9 The shape of the axial form factor F_A at low Q^2 using monopole, dipole, and quark model representations.

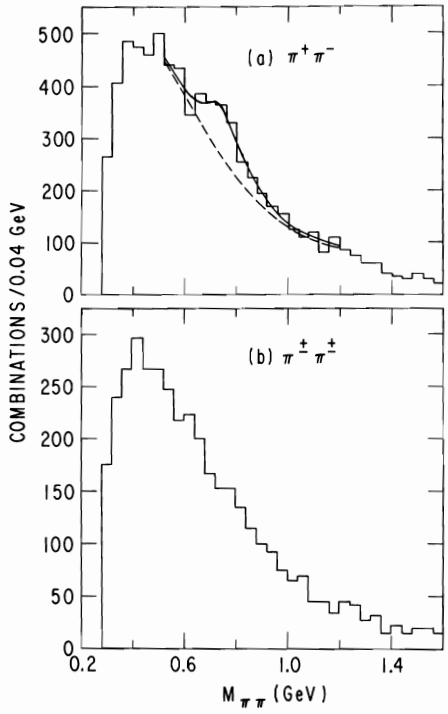

Fig. 10 The $\pi^+\pi^-$ and $\pi^\pm\pi^\pm$ effective mass distributions in the ACMP 15-ft antineutrino hydrogen experiment. The curves represent an incoherent sum of a quadratic background and a p-wave Breit-Wigner formula.

- Δ, N^* spectroscopy using neutrino beams is difficult. No individual Δ or N^* state has a cross section larger than 10% of the $\sigma(\Delta(1236))$.
- the low energy models do describe the new high energy data qualitatively.

Intermediate Mass Particles

The $\rho^o(760)$ has recently been seen in the inclusive process $\bar{\nu}p \to \mu^+\rho^oX$ by the Argonne-Carnegie-Mellon-Purdue 15-foot group.[11] Figure 10(a-b) shows the opposite sign and like sign $\pi\pi$ effective mass distributions. A clear $\rho^o(760)$ enhancement is seen. The rate can be given as ρ^o/event = 0.20 ± 0.03 or $\rho^o/\pi^- = 0.12 \pm 0.02$. However, the results are strong functions of various kinematic variables. Figure 11 shows the ρ^o production rate as a function of total hadronic mass. The number of ρ^o/event quickly rises to 35%. Figure 12(a-f) shows the ρ^o rate as a function of $P_\perp$ WRT $\vec{Q}$, $Z = E_H/(E_{\bar{\nu}} - E_\mu)$ and $Y_R = 1/2 \log[(E+P_\parallel)/(E-P_\parallel)]$. It can be seen that (1) the $P_\perp$ distribution of the ρ^o is flatter than that of the π^-, (2) 80% of the ρ^o's have $Z > 0.2$, which is often called the current fragmentation region, and (3) 70% of the ρ^o's have $Y_R > 0$, with an apparent peaking for $0.5 \leq Y_R \leq 1.0$. Some of these features of ρ^o production have also been observed in the process $\bar{\nu}N \to \mu^+\rho^-$, $(\rho^- \to \pi^-\pi^o)$ by the FMBH group in the 15-foot chamber.

Turning next to K^o production, similar results can be seen. Figure 13 shows the rate of K^o production as a function of W_{VIS} in νN interactions as measured by the Columbia-BNL 15-foot experiment[12]; the observed rate is quite similar to that of ρ^o production. Figure 14 shows the X_F distribution of

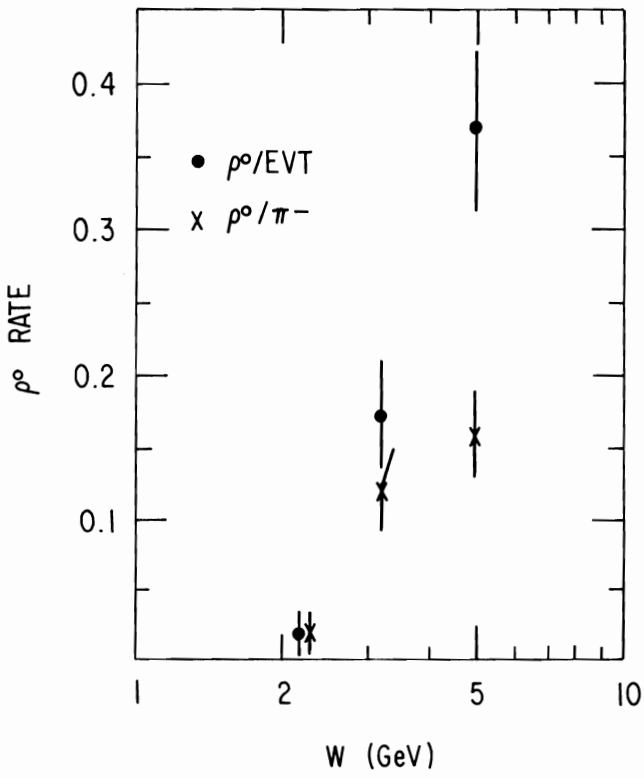

Fig. 11 The rate of $\rho^o(760)$ production in $\bar{\nu}p \to \mu^+$ as a function of hadronic mass. The data are from the ACMP 15-ft antineutrino hydrogen experiment.

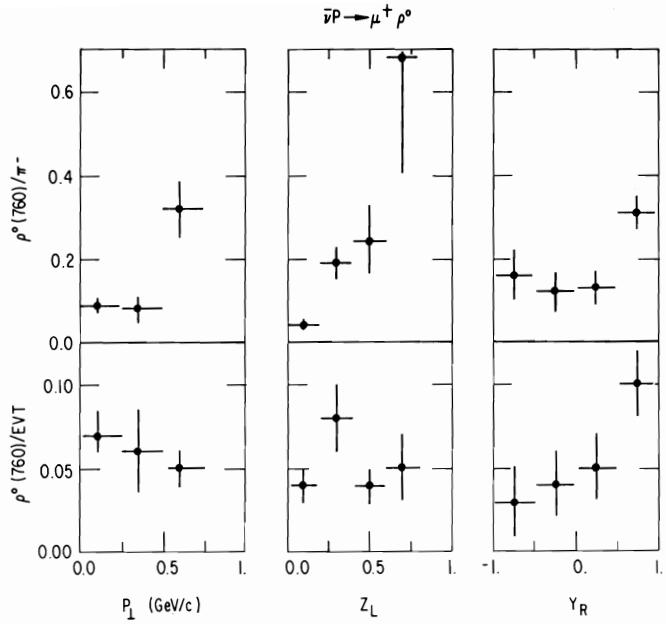

Fig. 12 In the process $\bar{\nu}p \to \mu^+\rho^o(760)$, the ratios ρ^o/event and ρ^o/π^- as a function of $P_\perp$, Z_L, and Y_R. The data are from the ACMP 15-ft antineutrino hydrogen experiment.

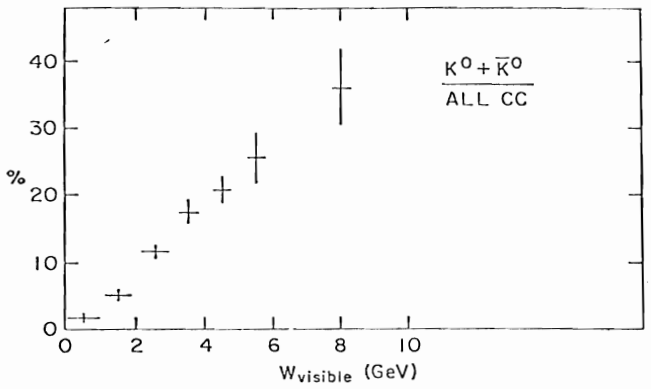

Fig. 13 The rate of K^o production as a function of W_{VIS} in the Columbia-BNL 15-ft neon experiment.

K^o's in $\bar{\nu}N$, νp, and $\pi^- p$ collisions.[13] The $\bar{\nu}N$ and νp data are very similar, but the $\pi^- p$ results (arbitrary normalization) also have a similar shape in the target fragmentation region. Presumably, associated production is the dominant mechanism in each case.

Finally, Fig. 15(a-b) displays the fragmentation functions D(z) for $K^o/\bar{K}^o$ in νN and $\bar{\nu}N$ interactions.[12,13] Their distributions are clearly broader than those of the pion. And it is interesting to note that for $z > 0.5$, $D^{\nu}_{K^o} \approx D^{\nu}_{\pi^-}$ and $D^{\bar{\nu}}_{\bar{K}^o} \approx D^{\bar{\nu}}_{\pi^+}$. This is not unexpected since one is observing the fragmentation of the up quark in the case of $\nu N \to \mu^- X$ and the fragmentation of the down quark in $\bar{\nu}N \to \mu^+ X$.

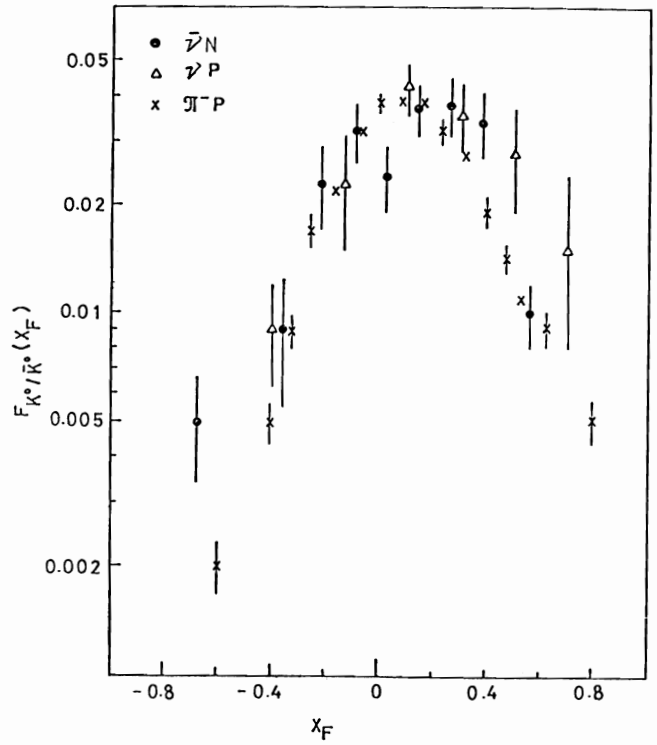

Fig. 14 The X_F distribution of K^o's in $\bar{\nu}N$ interactions as measured by the Serpukhov-Fermilab-Moscow-Michigan 15-ft experiment.

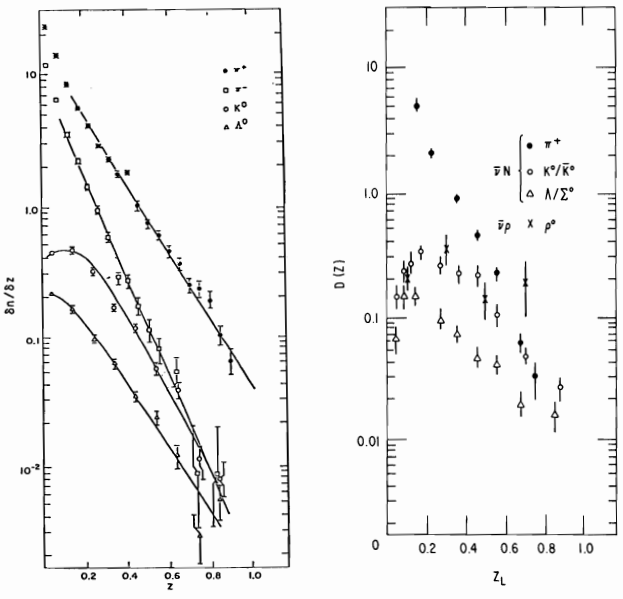

Fig. 15 The D(z) distributions in νN and $\bar{\nu}N$ interactions for K^o, Λ, and π as measured in the 15-ft chamber by the Columbia-BNL and SFMM groups.

Very little data has been reported on the production of K^* and Y^* resonances. Some rates for $K^*(890)$ and $Y^{*+}(1385)$ exist from the 15-foot broadband ν neon experiment, but nothing is known of their production mechanism. While there are detailed models[14] for the production of ρ, K^*, A_1, ω, η, ..., they have yet to be confronted with data.

High Mass Particle Production

The expression for the charged hadronic current in the standard QPM contains charm-changing and charm non-changing components:

$$J \propto \bar{u}\,[d \cdot \cos\theta + s \cdot \sin\theta] + \bar{c}\,[-d \cdot \sin\theta + s \cdot \cos\theta] \ .$$

It follows that neutrino beams can produce a charm meson or baryon by interactions off a valence quark in the nucleon, and in association with a strange particle, by interactions off a sea quark. Antineutrino beams, however, can only produce charm mesons by interactions off the sea quarks. In naive quark models, the expected charm particle rate is 5-10% for $\nu N \to \mu^-$ and 2-4% for $\bar{\nu} N \to \mu^+$. These rates are large. Neutrino interactions have always been viewed as a good process for discovering and studying the properties of charm mesons and baryons. In fact, e^+e^- interactions now seem to be the ideal place to study charm mesons. However, e^+e^- experiments have had difficulty in observing charmed baryons, and until this Conference, most of the data on charmed baryons has come from neutrino experiments. The remainder of this paper will be a review of the production rates of charm particles in $\nu N \to \mu X$ and attempts at doing charm baryon spectroscopy. Since dilepton production has been discussed by M. Murtagh at this Conference, I will concentrate on the strange particle tag for charm detection.

There is indirect evidence for charm particles in $\bar{\nu} p$ interactions as reflected in the inclusive strange particle distributions. Table III shows the expressions for $d^2\sigma/dxdy$, as calculated in the QPM, for various antineutrino processes. Events with no strange particles or with associated production of strange particles are seen to occur mainly at small y, with a valence x distribution. Events with charm occur mainly at small x, with a flat y distribution. The $\Delta S = -1$ events have a rate similar to that of charm and occur at small y with a valence x distribution. Thus, one would expect that charm production will yield an excess of strange particles at small x and large y as compared to the inclusive sample.

This hypothesis has been tested using $\bar{\nu} p \to \mu^+ V^o$ data from the Argonne-Carnegie-Mellon-Purdue 15-foot experiment.[15] The only strange particles detected are K_s^o and Λ decays, so to compare with the QPM, it was assumed that K^+ and K^o rates are equal and that the Λ, Σ^-, Σ^o, Σ^+ rates are equal. It was also assumed that the associated production of strange particles in $\bar{\nu} p$ collisions is given by the measured rate in non-weak lepton-nucleon interactions. And finally, the non-charm quark densities were taken from a popular model.[16]

Figure 16 displays the measured x and y distributions of Vees in $\bar{\nu} p \to \mu^+$ interactions; the curves correspond to the QPM with and without charm production. It is clear that the charmed hypothesis is favored. A fit to the x-y correlation yields $\chi^2/DF = 20/9$ for the prediction with charm and $\chi^2/DF = 60/9$ for the prediction without charm. One can use

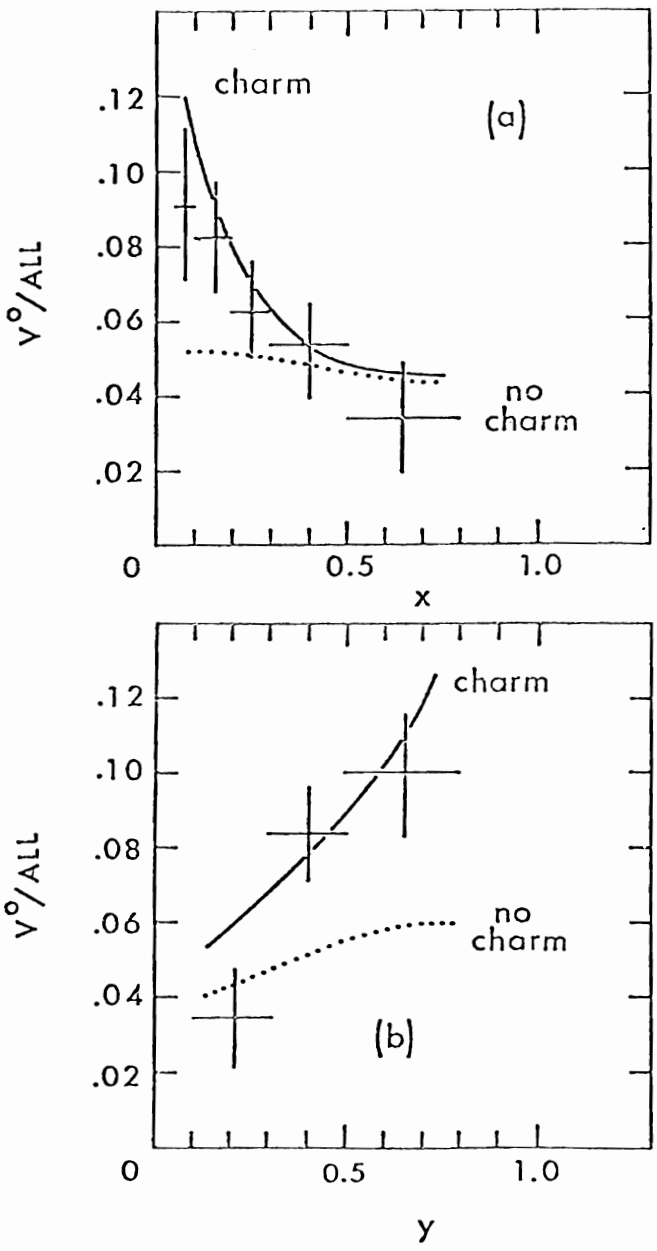

Fig. 16 The rate of K^o and Λ production as a function of x and y in $\bar{\nu} p \to \mu^+$ interactions as measured in the ACMP 15-ft experiment. The curves correspond to a QPM calculation with and without charm particle production.

this data to measure the following ratio of quark densities

$$\frac{\int x\,\bar{s}(x)\,dx}{\int x\,[0.343\,u(x) + \bar{d}(x) + \bar{s}(x)]\,dx} = 0.050 \pm 0.014$$

for $x \geq 0.05$ and $0.1 \leq y \leq 0.8$. This result is in reasonable agreement with sea quark measurements from dilepton experiments.

The dilepton events and the excess of strange particles at low x, high y are the only evidence for charm production by antineutrinos.

Table III: QPM Predictions for $\bar{\nu}p \to \mu^+$ Reactions

Process	$d^2\sigma/dxdy$	
$\bar{\nu}u \to \mu^+ d$	$x \cdot u(x) \cdot (1-y)^2 \cos^2\theta_c$	Non-Strange
$\bar{\nu}\bar{d} \to \mu^+ \bar{u}$	$x \cdot \bar{d}(x) \cdot \cos^2\theta_c$	+ Associated Production
$\bar{\nu}u \to \mu^+ s$	$x \cdot u(x) \cdot (1-y)^2 \sin^2\theta_c$	$\Delta S = -1$
$\nu\bar{s} \to \mu^+ \bar{u}$	$x \cdot \bar{s}(x) \cdot \sin^2\theta_c$	
$\bar{\nu}\bar{s} \to \mu^+ \bar{c}$	$x \cdot \bar{s}(x) \cdot \cos^2\theta_c$	$\Delta C = -1$
$\bar{\nu}\bar{d} \to \mu^+ \bar{c}$	$x \cdot \bar{d}(x) \cdot \sin^2\theta_c$	

Explicit Charm Particle Rates

Direct evidence for charm particles in effective mass distributions and in constrained, exclusive final states come from four bubble chamber experiments.

Inclusive $D^o(1860)$ Rate: The first observation of the D^o in neutrino reactions was made by the Columbia-BNL, 15-foot heavy neon broad-band ν beam experiment last year.[17] The group has now processed nearly twice as much film and have an updated result on the D^o rate.[12] In 106,000 CC events (134,000 pictures), all K^o_s and Λ decays were analyzed and effective mass combinations with the quantum numbers of the D^o were inspected. No D^+ signal is seen, but a peak in the $K^o_s\pi^+\pi^-$ spectrum at 1850 ± 15 MeV is seen. After correcting for K^o detection efficiency, the following rate is observed:

$$\frac{\nu N \to \mu^- D^o \hookrightarrow K^o\pi^+\pi^-}{\nu N \to \mu^-} = (0.40 \pm 0.15)\% \quad .$$

If one uses a $D^o \to K^o\pi^+\pi^-$ branching ratio of 4.0% (not well known), then the inclusive D^o rate in νN interactions near 25 GeV beam energy is (10 ± 4)%.

$D^{*+}(2010)$ Rate: The Aachen-Bonn-CERN-Munich-Oxford broad-band νH_2 experiment[18] using the BEBC chamber has recently observed the D^{*+} in νp charged-current interactions. They first searched for three-constraint kinematic fits in their data sample of 6500 events to $\Delta S = -\Delta Q$ final states. Two candidates were found. The first is an example of $\nu p \to \mu^- pK^-\pi^+\pi^+$ at 47.8 GeV neutrino energy. The K^- is identified by means of ionization, energy loss, and a secondary scatter. The following mass values were observed: $M(K^-\pi^+\pi^+) = 2011 \pm 6$, $M(K^-\pi^+) = 1865 \pm 4$, and $\Delta M = M(K^-\pi^+\pi^+) - M(K^-\pi^+) = 145.2 \pm 0.5$ MeV. The current best value for the $D^{*+} - D^o$ mass difference from e^+e^- experiments is 145.3 ± 0.5 MeV. Thus this event is a good candidate for $\nu p \to \mu^- pD^{*+}$. There is background to the event due to the possible $\nu p \to \mu^- pK^-\pi^+\pi^- K^o_L$ and $\nu p \to \mu^- K^+K^-\pi^+\pi^+ n$ hypotheses, which cannot be excluded. The total background is only 0.04 events and therefore the event is a highly probable $\Delta S = -\Delta Q$ event.

The second event is an example of $\nu p \to \mu^- pK^- + 4\pi^+ + 2\pi^-$ at 21.3 GeV neutrino energy. The K^- is identified by means of a secondary matter. The following mass values were observed: $M(K^-\pi^+\pi^+\pi^+\pi^-) = 2013 \pm 4$, $M(K^-\pi^+\pi^+\pi^-) = 1868 \pm 4$, and $\Delta M = 145.2 \pm 0.6$ MeV. There is, of course, background to the event from possible associated production hypotheses; the total background is 10^{-4}, and therefore the event is a highly probable example of $\nu p \to \mu^- pD^{*+}\pi^+\pi^-$.

These two events establish that the $D^*(2010)$ rate is finite and possibly large since the above-mentioned analysis is sensitive to only exclusive channels with no missing neutrals. To get a better estimate of the true D^* rate, the experiment exploits the fact that the mass resolution in $M(D^{*+}) - M(D^o)$ is ~ 3 MeV. The mass difference is calculated for the combinations $(K^-\pi^+)\pi^+$, $(K^-\pi^+\pi^+\pi^-)\pi^+$, and $(K^o_s\pi^+\pi^-)\pi^+$ whenever $M(K\ell\pi) = 1865 \pm 25$ MeV. For the first two of the above combinations, all negative tracks are called K^- even if they cannot be identified as K^- by means of energy loss, ionization, etc. Fig. 17 shows the measured ΔM distributions. There is a possible signal in each combination. From the summed distribution, one obtains 7 ± 4 $D^{*+} \to D^o$ events (where 2 of the 7 are the exclusive events). Correcting for K^o, D^o, and D^{*+} detection efficiencies and branching ratios, the experiment obtains the rate

$$\frac{\nu p \to \mu^- D^{*+}}{\nu p \to \mu^- X \,|\, W > 2.9 \text{ GeV}} = (4.1 \pm 2.4)\% \quad .$$

Charm Baryons: Two light liquid bubble chamber experiments have observed the $\Lambda_c^+(2260)$ in exclusive final states. As always in these kind of studies, one is restricted to events giving three-constraint kinematic fits with no missing neutrals.

The first neutrino-induced Λ_c^+ event was seen by the BNL group[19] in the 7-foot chamber in 1975. It is an example of

$$\nu p \to \mu^- \Sigma_c^{++} \hookrightarrow \Lambda_c^+\pi^+ \hookrightarrow \Lambda\pi^+\pi^+\pi^-$$

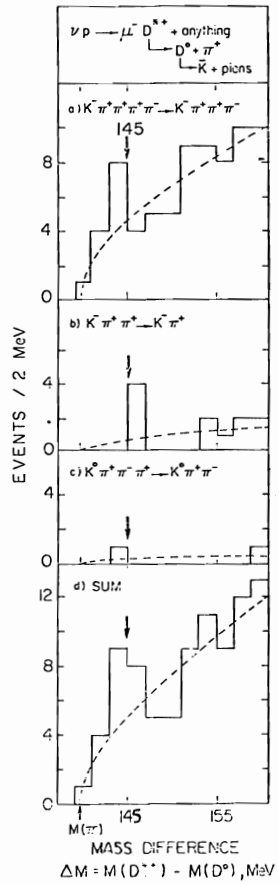

Fig. 17 The $\Delta M = M(D^{*+}) - M(D^{o})$ distributions for various D^{o} decay modes as measured by the ABCMO experiment using BEBC.

at 13.5 GeV beam energy. The $M(\Lambda\pi^+\pi^+\pi^-)$ value is 2260 ± 10 MeV. Four years later, a second event was found in the BNL experiment[20] of the type

$$\nu d \to \mu^- \Lambda_c^+(p_s) \quad \Lambda_c^+ \to K_s^o p\pi^+\pi^-$$

at 4 GeV beam energy. The following mass values were measured: $M(K_s^o\pi^-) = 913 \pm 8$ and $M(\bar{K}^o p\pi^+\pi^-) = 2254 \pm 12$ MeV. It is probable that the $K_s^o\pi^-$ system is a $K^{*-}(890)$ and therefore the strangeness of the event is fixed at -1. The μ^- track is identified by penetration of three 2-inch thick steel plates; the π^- track interacts in one of the plates. The fast proton is identified by ionization; the π^+ track is not a K^+ or proton because of energy loss. The three associated production hypotheses $\nu n \to \mu^- pK_s^o K_s^o$, $\nu n \to \mu^- pK^-\pi^+$, and $\nu n \to \mu^- pK_s^o\pi^+\pi^- K_L^o$ cannot be excluded, but their total background contribution is estimated to be only 0.012 events.

To determine a rate for Λ_c^+ production based on these two events, one notes that of the 5200 events in the 1.1×10^6 pictures, only 700 have beam energies above the Λ_c^+ threshold energy. Correcting for K^o and Λ detection efficiency, but not for the unknown Λ_c^+ branching ratios, one obtains a rate for Λ_c^+ production with no missing neutrals of $(0.9 \pm 0.7)\%$ for $E_\nu \geq 4$ GeV.

The second experiment[21] to see exclusive charm baryon events is the Tohoku-IIT-Maryland-Stonybrook-Tufts (TIMST) ν-D_2 experiment in the 15-foot chamber at Fermilab. This new experiment used a broad-band neutrino beam of $\sim$ 25 GeV. They have reported preliminary results from 150,000 of their 328,000 pictures. In 10,000 charged-current events, all events with an associated K_s^o or Λ decay were processed and fits tried to $\Delta S = -\Delta Q$ hypotheses; four candidates were found.

The best candidate is an example of

$$\nu d \to \mu^- \Lambda_c^+ \pi^+\pi^-(p_s) \quad \Lambda_c^+ \to \Lambda\pi^+\pi^+\pi^- ,$$

where $M(\Lambda\pi^+\pi^+\pi^-) = 2257 \pm 17$, $M(\Lambda\pi^-) = 1382 \pm 3$, and $M(\Lambda\pi^+\pi^+\pi^-\pi^+) = 2486 \pm 19$ MeV. So there is a suggestion that the following cascade has occurred: $\Sigma_c^{*++} \to \Lambda_c^+\pi^+$, $\Lambda_c^+ \to Y^{*-}\pi^+\pi^+$, $Y^{*-} \to \Lambda\pi^-$. All of the final state pions have momenta ≤ 0.74 GeV/c and ionization favors the pion mass assignment over the kaon mass in each case. The probability of a missing K^o in the final state is only $\sim 5 \times 10^{-3}$. Thus the event is a solid Λ_c^+ production candidate.

The other three candidates in the experiment are not as clean since associated production hypotheses cannot be excluded with high probability. However, they are useful to look at since they do provide an indication of rates. Event 2 is possibly a second example of $\nu d \to \mu^- \Lambda_c^+\pi^+\pi^-(p_s)$ at 14.4 GeV beam energy. The relevant mass values are $M(\Lambda\pi^+\pi^+\pi^+\pi^-) = 2509 \pm 13$ and $M(\Lambda\pi^+\pi^+\pi^-) = 2256 \pm 12$ MeV. However, the event also fits the hypotheses $\nu d \to \mu^- \Lambda K^+\pi^+\pi^+\pi^-\pi^-$ and, furthermore, the probability of a missing K_L^o is 6%.

Event 3 is a candidate for the reaction $\nu d \to \mu^- \Lambda_c^+(p_s)$, with $\Lambda_c^+ \to \Lambda\pi^+$. The beam energy is 22.8 GeV and $M(\Lambda\pi^+) = 2266 \pm 8$ MeV. The event also fits the hypothesis $\nu d \to \mu^- \Lambda K^+(p_s)$. In fact, there are 14 events in the experiment which fit that associated production reaction; if the K^+ track is called a π^+ in each event, then there is no other resulting "$\Lambda\pi^+$" effective mass within 100 MeV of $M(\Lambda_c^+)$. So Event No. 3 must be viewed as a serious Λ_c^+ candidate, but one must await more detailed background calculations. The final candidate, Event 4, is consistent with the hypothesis $\nu d \to \mu^- \Lambda_c^+\pi^+(n_s)$ with $\Lambda_c^+ \to K_s^o p\pi^+\pi^-$. The beam energy is 18.3 GeV and $M(pK_s^o\pi^+\pi^-) = 2246 \pm 6$, $M(K_s^o\pi^-) = 914 \pm 5$, and $M(p\pi^+) = 1211 \pm 5$ MeV. So there is a suggestion that the following cascade has occurred: $\Lambda_c^+ \to K_{890}^{*-}\Delta_{1236}^{++}$. But once again, it is not possible to exclude all associated production hypotheses.

One concludes that the 15-foot νD_2 experiment has observed between 1 and 4 events of Λ_c^+ production in 10,000 events, with three of the candidates being off a neutron target. Thus the rate of exclusive channel charm production is very low; one will need 10^5 event experiments to do detailed studies of charm reactions.

Since exclusive charm rates are so small, one next turns to the inclusive mode in hope of detecting a larger signal. Figure 18 shows the inclusive $\Lambda\pi^+$ mass distribution from the TIMST experiment.[22] To enhance any Λ_c^+ signal, a selection was made that

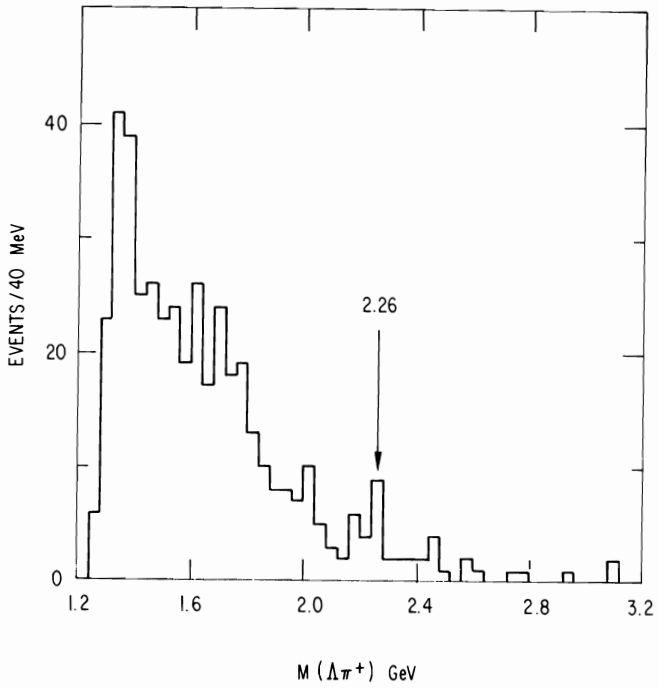

Fig. 18 The $\Lambda\pi^+$ effective mass distribution with the selection $\cos\theta_\Lambda > -0.75$ as measured in the Tohoku-IIT-Maryland-Stony Brook-Tufts collaboration neutrino-deuterium experiment.

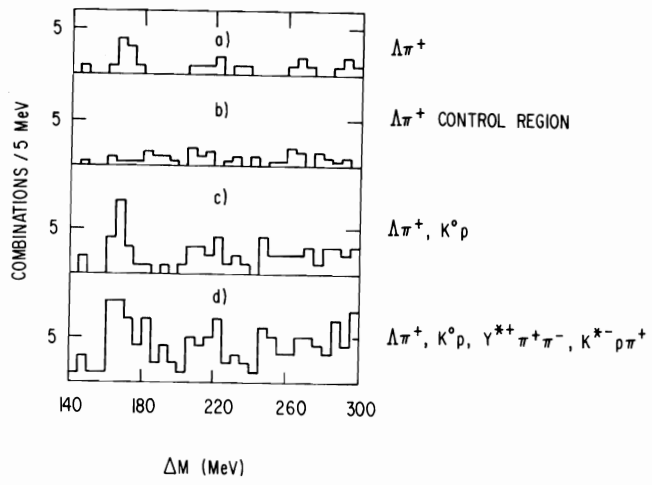

Fig. 19 The $\Delta M = M(\Sigma_c^{++}) - M(\Lambda_c^+)$ distributions for various Λ_c^+ decay modes as measured by the Columbia-BNL 15-ft experiment.

$\cos\theta_{\Lambda^+} > -0.75$ where θ is calculated in the $\Lambda\pi^+$ rest frame with respect to the $\Lambda\pi^+$ line of flight. A possible enhancement is seen at $\sim$ 2260 MeV. After the remainder of the group's 328K pictures are processed, this distribution could contain a quite significant Λ_c^+ signal above a fairly low background.

A clear inclusive Λ_c^+ signal is certainly seen by the Columbia-BNL 15-foot hydrogen-neon experiment.[23] They do not see any convincing mass peaks for the Λ_c^+ in uncut distributions, but they see evidence for the decay chain $\Sigma_c^{++} \to \Lambda_c^+\pi^+$, $\Lambda_c^+ \to$ (Λ + charged pions) or ($K_s^o p$ + charged pions). They select $\Lambda\pi^+$, $K_s^o p$, $Y^{*+}\pi^+\pi^-$, $K^{*-}p\pi^+$ particle combinations, with $2235 \leq M \leq 2285$ MeV, when there is another π^+ in the event. Then the corresponding mass differences are histogrammed, as shown in Fig. 19(a, c, d); an enhancement is present near 166 MeV. The resolution is ±3 MeV. Fig. 19(b) shows the $\Lambda\pi^+\pi^+ - \Lambda\pi^+$ mass difference when $M_{\Lambda\pi^+} \neq M_{\Lambda_c}$ and no enhancement is evident. Selecting events with $\Delta M = 166 \pm 6$ MeV, Fig. 20(a, c, d) shows the corresponding effective mass combinations with the quantum numbers of the Λ_c^+. A total of 14 events over a background of 6 are seen at 2260 MeV in Fig. 20(d). Fig. 20(b) again is a control region where $\Delta M = 154 \pm 6$ or 178 ± 6 MeV; no peaking is present in the 2200-2300 MeV region. Table IV gives the $\Sigma^{++} \to \Lambda_c^+$ event rate in each of the four decay modes considered; the probability of the enhancement in Fig. 20(d) being a statistical fluctuation is 10^{-5}.

Note that the $K^{*-}_{890}\,\Delta^{++}$ decay mode of the Λ_c^+ is apparently small; at least one model for Λ_c^+ branching fractions has predicted that this two-body resonance channel would be quite large compared to other detectable modes.

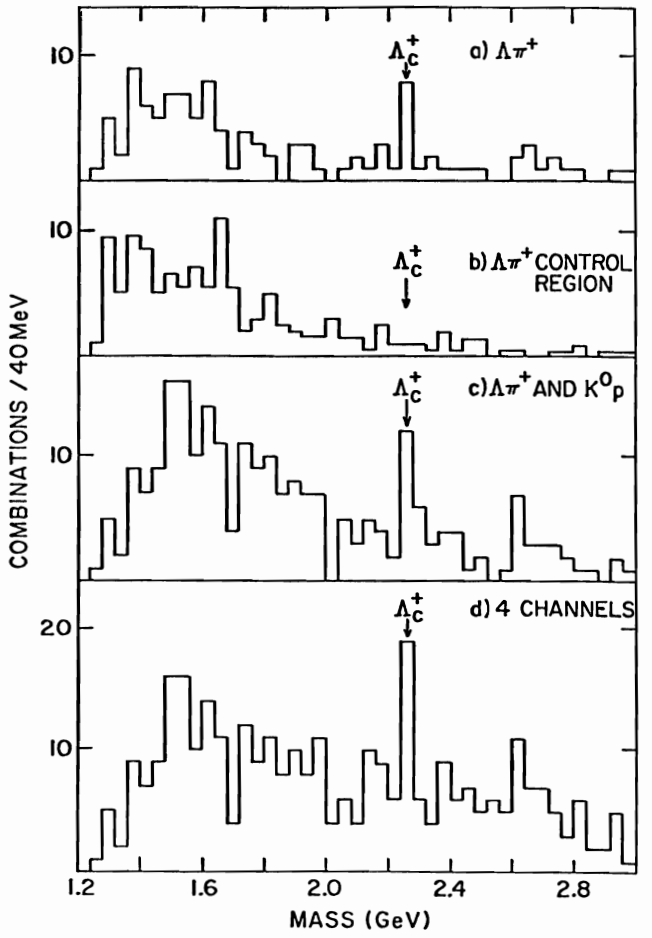

Fig. 20 Effective mass distributions with the quantum numbers of the Λ_c^+ with the selection that $\Delta M = 166 \pm 6$ MeV. Data from the Columbia-BNL 15-ft experiment.

Table IV: Columbia-BNL $\nu N \to \Sigma_c^{++} \to \Lambda_c^+ \pi^+$ Results[23]

Λ_c^+ Decay Mode	Events	Background	Corrected Signal	$\sigma \cdot B/\sigma_{cc}$
$\Lambda\pi^+$	8	1.5	17.6	$1.8 \pm 0.8 \times 10^{-4}$
$\bar{K}^o p$	7	2.0	25.5	2.7 ± 1.6
$Y^{*+}\pi^+\pi^-$	4	1.5	12.4	1.5 ± 1.4
$K^{*-}p\pi^+$	1	1.0		
	20	6.0	55.5	$6 \pm 2.3 \times 10^{-4}$

Finally, it is of interest to note that only one of the above discussed 14 $\Sigma_c^{++} \to \Lambda_c^+\pi^+$ events is a serious candidate for the quasielastic process $\nu p \to \mu^- \Sigma_c^{++}$. The observed Σ_c^{++} decay mode is $\Lambda_c^+\pi^+$ followed by $\Lambda_c^+ \to \Lambda\pi^+\pi^+\pi^-$. All three of its positive tracks are pions from range, energy loss, or ionization. There are no associated K_L^o or neutrons in 2.5 interaction lengths of neon; and there are no associated gammas in 7 radiation lengths. The event balances transverse momentum to 70 MeV/c. The group concludes that the probability that the event is associated production is only ~ 3%.

The only detailed theoretical predictions for charm baryon production by neutrinos are for exclusive channels. Table V gives cross section predictions, at 10 GeV beam energy, for $\nu n \to \mu^- \Lambda_c^+$ and $\nu p \to \mu^- \Sigma_c^{++}$, Σ_c^{*++} as calculated by four models.[24-27] There are rather large differences in the predictions. It is difficult to compare the available data (~ 3 events) with these numbers because the Λ_c^+ branching ratios are not known. If one assumes a Σ_c^{++}, Σ_c^{*++} detection efficiency of 10%, then the combined H_2/D_2 data from the 7-foot, 15-foot, and BEBC give $\sigma(\nu p \to \mu^- \Sigma_c, \Sigma_c^*) \sim 1 \times 10^{-40}$ cm^2 and the Columbia-BNL 15-foot event in neon corresponds to ~ 0.4×10^{-40} cm^2. It is clear that unless there are few Λ_c^+ decay modes with no π^o's or neutrons, the exclusive channel cross sections are smaller than many people had expected.

Summary of Charm Production: One can use the eight $\Delta S = -\Delta Q$ exclusive candidates to study the production kinematics of charm particles. Fig. 21 shows the x, y, and Q^2 distributions for the eight events. They have the expected valence x distribution. And since the events are generally quasi two- and three-body final states, it is not surprising that they are at fairly low Q^2 values.

To determine the mass of Λ_c^+, I have averaged the mass values from the four "best" (lowest background) $\Delta S = -\Delta Q$ exclusive events: the two 7-foot events, the νD_2 15-foot event, and the ν neon 15-foot event. The result is 2259 ± 7 MeV. The Columbia-BNL inclusive $\Lambda_c^+ \to \Lambda\pi^+$ events yield the value of 2257 ± 10 MeV.

Table VI is a comparison between experiments that observe a charm particle signal and those that do not. Inclusive $D^o \to K_s^o\pi^+\pi^-$, inclusive $\Sigma_c^{++} \to \Lambda_c^+\pi^+$, exclusive D^{*+}, and exclusive Λ_c^+ rates are compared by giving the observed raw, uncorrected rates, and the number of events one expects in the other experiments. Note that the two BNL 7-foot Λ_c^+ events are seen in a fairly low energy experiment; to compare

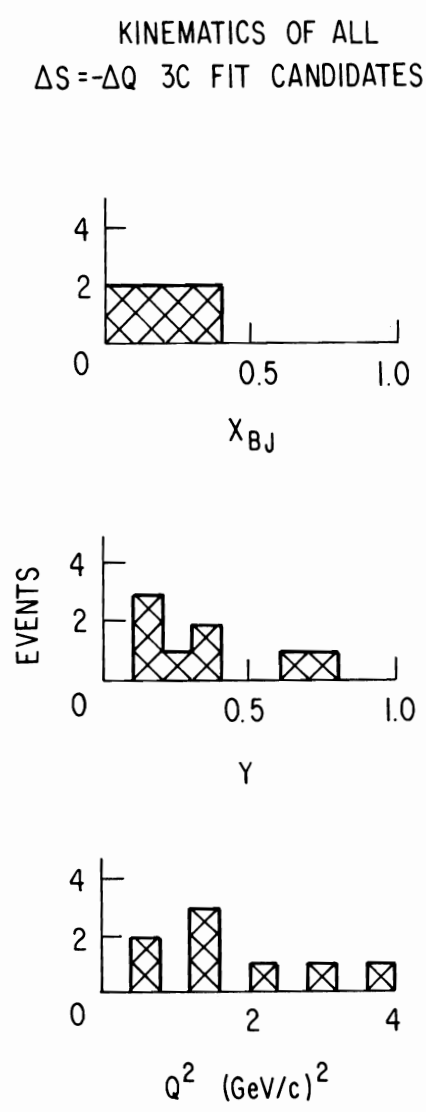

Fig. 21 The x, y, and Q^2 distributions for the eight $\Delta S = -\Delta Q$ neutrino events.

Table V: Exclusive Charm Baryon Rates

Model	$\sigma(E_\nu = 10\ \text{GeV})\ 10^{40}\ \text{cm}^2$	
	$\nu n \to \mu^- \Lambda_c^+$	$\nu p \to \mu^- \Sigma_c^{++}$, $\mu^- \Sigma_c^{*++}$
Lee-Shrock[24] SU(4) Symmetry for Couplings D^* Dominated Dipole Form Factors	23	25
Amer et al.[25] Quark Model + SU(4) Breaking	3.2	
Finjoird-Ravndal[26] Quark Model + "Nucleon" Form Factors	1.2	0.8
Avilz-Kobayashi-Körner[27] QM: 1977 $m_c = m_d$	30	15
1979 $m_c \neq m_d$	7.5	2.5

Table VI: Comparison of Raw (uncorrected) Charm Rates
High Energy ν Bubble Chamber Experiments;
All Rates Have Errors in 20-80% Range

Chamber	BEBC	15-foot			7-foot
Liquid	H_2	H_2	D_2	Neon	H_2/D_2
CC Events > 4 GeV	6000	2500	8000	100,000	700
$\langle E_\nu \rangle$	30	25	25	30	6
Observed Inc. $D^o \to K_s^o \pi^+ \pi^-$	No	No	No	$R = 1.4 \times 10^{-3}$	
Expected/BG Events	6/20	3/2	8/26		
Observed Inc. $\Sigma_c^{++} \to \Lambda_c^+ \pi^+$	No	No	No	$R = 1.5 \times 10^{-4}$	
Expected Events	$\lesssim 1$	$\lesssim 1$	$\lesssim 1$-2		
Observed Exc. D^{*+}	2 events ($R = 3 \times 10^{-4}$)	No	---	---	
Expected Events		$\lesssim 1$			
Observed Exc. Λ_c^+	No	No	$\sim$ 2 events ($R = 4 \times 10^{-4}$)	1 event ($R = ?$)	2 events ($R = 3 \times 10^{-3}$)
Expected Events if $R = 4 \times 10^{-4}$	2	$\lesssim 1$			
Expected Events if $R = 3 \times 10^{-3}$ and $\sigma_{\Lambda_c^+}$ Constant ≥ 4 GeV	5	2			

with the high energy data, I have assumed an exclusive channel cross section independent of beam energy above 4 GeV. Overall, there are no serious conflicts between the five experiments. But there is no inclusive or exclusive rate that has been confirmed by a second experiment.

It is clear that charm baryon spectroscopy is difficult with present day neutrino beams and detectors. As suggested by the dilepton data, much of the neutrino flux in the broad-band beams is at energies where the charm rate is slowly rising from threshold. The use of a much higher energy beam from the Tevatron would be of great value to charm spectroscopy.

This research was supported by the U. S. Department of Energy.

References

1. S. J. Barish et al., Argonne-Carnegie-Mellon-Purdue collaboration, ANL-HEP-PR-78-30.
2. M. Pohl et al., Nuovo Cimento 24, 540 (1979).
3. T. Bolognese et al., GGM propane-freon collaboration, CRN/HE 78-26.
4. J. Blielschau et al., Aachen-Bonn-CERN-Munich-Oxford collaboration, paper submitted to this Conference.
5. J. Bell et al., Phys. Rev. Letters 41, 1008 (1978).

6. S. J. Barish et al., Argonne-Carnegie-Mellon-Purdue collaboration, paper submitted to this Conference.
7. S. Adler, Ann. of Physics 50, 89 (1968) and Phys. Rev. D12, 2644 (1975).
8. G. L. Fogli and G. Nardulli, Istituto di Fisica-Bari preprint (1979).
9. F. Ravndal, Nuovo Cimento 18A, 385 (1973).
10. P. Andreadis et al., Ann. of Phys. 88, 242 (1974).
11. M. Derrick et al., Argonne-Carnegie-Mellon-Purdue collaboration, paper submitted to this Conference.
12. C. Baltay, private communication.
13. V. Ammosov et al., Serpukhov-Fermilab-Moscow-Michigan collaboration, Fermilab-PUB 79/15-EXP.
14. A. Bartl et al., paper submitted to this Conference.
15. S. J. Barish et al., Argonne-Carnegie-Mellon-Purdue collaboration, paper submitted to this Conference.
16. R. Field and R. Feynman, Phys. Rev. D15, 2590 (1977).
17. C. Baltay et al., Phys. Rev. Letters 41, 73 (1978).
18. J. Blietschau et al., Aachen-Bonn-CERN-Munich-Oxford collaboration, CERN/EP 79-60.
19. E. G. Cazzoli et al., Phys. Rev. Letters 34, 1125 (1975).
20. A. M. Cnops et al., Phys. Rev. Letters 42, 197 (1979).
21. T. Kitagaki et al., Tohoku-Illinois Institute of Technology-Maryland-Stony Brook-Tufts collaboration, paper submitted to this Conference.
22. T. Kitagaki, private communication.
23. C. Baltay et al., Phys. Rev. Letters 42, 1721 (1979).
24. R. Shroch and B. Lee, Phys. Rev. D13, 2539 (1976).
25. J. Finjord and F. Ravndal, Phys. 58B, 61 (1975).
26. C. Avilez et al., Phys. Letters 66B, 149 (1977); Phys. Rev. D17, 709 (1978); Phys. Rev. D19, 3448 (1979).
27. A. Amer et al., Phys. Letters 81B, 48 (1979).

Questions

F. Messing
Carnegie-Mellon

I have more a comment than a question. There was a question raised earlier about the helicity of charmed particle production. I'd just like to point out that the rise in strange particle production with y makes an inescapable conclusion that there is a strong left-handed component in charmed particle production. If you assume a full strength charmed particle production, then the size of the $\bar{s}$ sea agrees with that measurement in the dileptons.

G. Snow
Maryland

I have a question about what can one say about single strange baryon production, not charmed baryon production, just the simple Cabibbo antineutrino nucleon goes to a single strange baryon.

P. Schreiner
ANL

Like $\bar{\nu} p \rightarrow \mu^+ \Lambda$? - Yes. Some events have been observed. The Gargamelle experiment has a sample, I think, of about 30 events in propane and freon for that reaction, and the Argonne/Carnegie-Mellon/Purdue 15' antineutrino experiment has about a half dozen $\bar{\nu} p \rightarrow \mu^+ \Lambda$ events, but they are very difficult to see.